Theoretical Study on the Origin of Enantioselectivity in the Bis(dihydroquinidine)-3,6-pyridazine·Osmium Tetroxide-Catalyzed Dihydroxylation of Styrene

Gregori Ujaque, Feliu Maseras,* and Agustí Lledós

Contribution from the Unitat de Química Física, Edifici C.n, Universitat Autònoma de Barcelona, 08193 Bellaterra, Catalonia, Spain

Received May 11, 1998

Abstract: The origin of enantioselectivity in the dihydroxylation of $H_2C{=}CH(Ph)$ catalyzed by $(DHQD)_2PYDZ{\cdot}OsO_4$ ($(DHQD)_2PYDZ$ = bis(dihydroquinidine)-3,6-pyridazine) is analyzed theoretically by means of hybrid QM/MM calculations with the IMOMM(Becke3LYP:MM3) method. Twelve different possible reaction paths are defined from the three possible regions of entry of the substrate and its four possible orientations and characterized through their respective transition states. The transition state with the lowest energy leads to the R product, in agreement with experimental results. The decomposition of the interaction energy between catalyst and substrate shows how the selectivity is essentially governed by stacking interactions between aromatic rings, with a leading role for the face-to-face interaction between the substrate and one of the quinoline rings of the catalyst.

Introduction

The osmium-catalyzed dihydroxylation of olefins is a powerful method for the enantioselective introduction of chiral centers in organic substrates.[1,2] The key step of the reaction, where the chirality of the diol product is decided, is the formation of a cyclic osmate ether intermediate. The detailed mechanism of formation of this intermediate has been obscure for a long time,[3−6] and only recently is a consensus emerging in favor of the so called [3 + 2] model, where the reaction takes place through a concerted cycloaddition of two oxygens to the olefin bond. Theoretical ab initio studies on the $OsO_4(NH_3)$ + $H_2C{=}CH_2$ model system have been determinant in the creation of this consensus, because they predict a difference of *ca*. 200 $kJ{\cdot}mol^{-1}$ between the [3 + 2] mechanism and the alternative [2 + 2] mechanism.[7−10] Other recent support for the [3 + 2] mechanism has come from a critical analysis of available experimental data,[11] and from new measurements of kinetic isotope effects.[10,12]

Despite its undisputable relevance, the preference for the [3 + 2] model does not provide in itself an explanation to the stereoselectivity of the reaction. One can indeed have both enantiomers via the [3 + 2] mechanism. Studies published so far on the origin of stereoselectivity are mostly of a qualitative nature. The analysis by Corey and Noe[11] mentioned above is based essentially on the geometrical features of the catalysts and the space available for placement of the substrate. Houk and co-workers[13] and Sharpless and co-workers[14] have published pure molecular mechanics studies on the problem that compute the correct stereoselectivity. Their predictive power is however questionable because of a certain arbitrariness in the geometry of the reaction center, which is frozen in one case,[13] and computed with force field parameters based on the validity of the [2 + 2] model in the other case.[14] Another recent pure DFT study[15] on the $OsO_4(NH_3)$ + $H_2C{=}CH(CH_2OH)$ reaction draws its interest from the comparison with purely organic systems, but touches only marginally the topic of enantioselectivity, which is governed in experimental systems by the nature of the bulky cinchona alkaloid attached to the metal.

The goal of the present paper is to provide a quantitative theoretical characterization of the origin of enantioselectivity in the osmium-catalyzed dihydroxylation of olefins. To accomplish it, we have carried out IMOMM calculations on the $(DHQD)_2PYDZ{\cdot}OsO_4$ (**1**) + $H_2C{=}CH(Ph)$ (**2**) system. IMOMM is a hybrid method mixing quantum mechanics and molecular mechanics descriptions for different parts of the system,[16] the performance of which has been already tested in a satisfactory way for a number of transition metal systems.[17−20] In particular, we have already applied it to the study of two

(1) Kolb, H. C.; VanNieuwenhze, M. S.; Sharpless, K. B. *Chem. Rev.* **1994**, *94*, 2483.
(2) Lohray, B. B. *Tetrahedron: Asymmetry* **1992** *3*, 1317.
(3) Göbel, T.; Sharpless, K. B. *Angew. Chem., Int. Ed. Engl.* **1993** *32*, 1329.
(4) Corey, E. J.; Guzman-Perez, A.; Noe, M. C. *J. Am. Chem. Soc.* **1995**, *117*, 10805.
(5) Corey, E. J.; Guzman-Perez, A.; Noe, M. C. *J. Am. Chem. Soc.* **1995**, *117*, 10817.
(6) Norrby, P.-O.; Gable, K. P. *J. Chem. Soc., Perkin Trans. 2* **1995**, 171.
(7) Dapprich, S.; Ujaque, G.; Maseras, F.; Lledós, A.; Musaev, D. G.; Morokuma, K. *J. Am. Chem. Soc.* **1996**, *118*, 11660.
(8) Pidun, U.; Boehme, C.; Frenking, G. *Angew. Chem., Int. Ed. Engl.* **1996**, *35*, 2817.
(9) Torrent, M.; Deng, L.; Duran, M.; Sola, M.; Ziegler, T. *Organometallics* **1997**, *16*, 13.
(10) DelMonte, A. J.; Haller, J.; Houk, K. N.; Sharpless, K. B.; Singleton, D. A.; Strassner, T.; Thomas, A. A. *J. Am. Chem. Soc.* **1997**, *119*, 9907.
(11) Corey, E. J.; Noe, M. C. *J. Am. Chem. Soc.* **1996**, *118*, 11038.
(12) Corey, E. J.; Noe, M. C.; Grogan, M. J. *Tetrahedron Lett.* **1996**, *37*, 4899.
(13) Wu, Y.-D.; Wang, Y.; Houk, K. N. *J. Am. Chem. Soc.* **1992**, *57*, 1362.
(14) Norrby, P.-O.; Kolb, H. C.; Sharpless, K. B. *J. Am. Chem. Soc.* **1994**, *116*, 8470.
(15) Haller, J.; Strassner, T.; Houk, K. N. *J. Am. Chem. Soc.* **1997**, *119*, 8031.
(16) Maseras, F.; Morokuma, K. *J. Comput. Chem.* **1995**, *16*, 1170.

10.1021/ja9816335 CCC: $18.00
Published on Web 01/27/1999

Chart 1

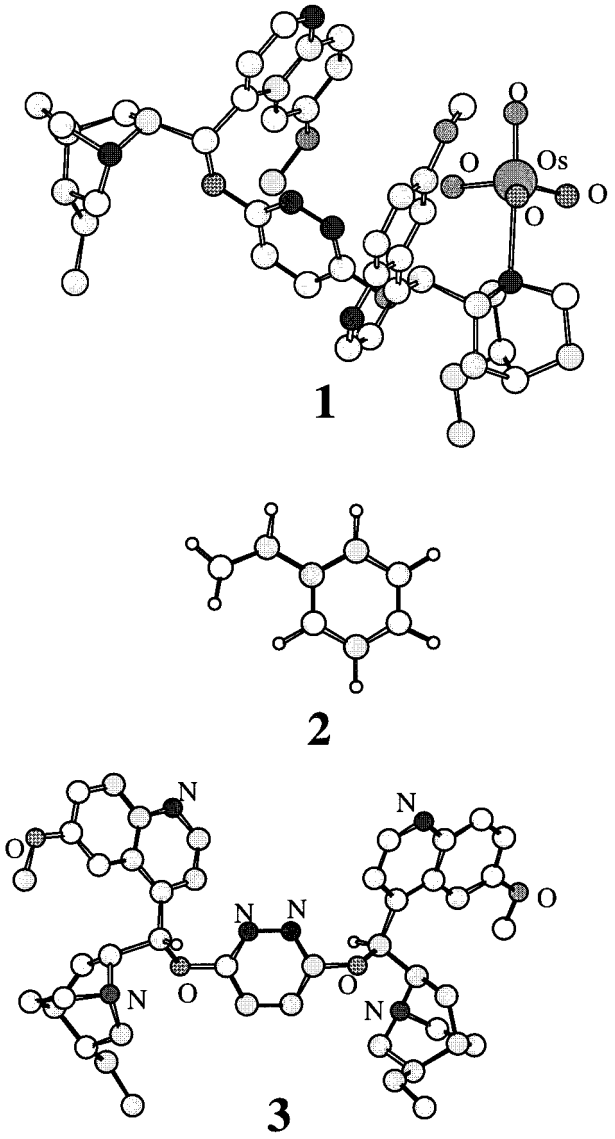

closely related problems: the structural features of [OsO_4(quinuclidine)] and [OsO_4{dimethylcarbamoyl)dihydroquinidine}],[19] and the characterization of an intermediate for the same reaction **1** + **2** studied in this paper.[20]

The system we study in this paper, **1** + **2**, has been the object of a number of experimental studies by Corey and coworkers.[11,21] The catalyst belongs to the so called second generation,[1] with the alkaloid ligand **3** having a "dimeric" form based on a heterocyclic spacer, in this case pyridazine. The substrate, styrene, has been proved experimentally to show high selectivity with this catalyst, giving in particular an enantiomeric excess of 96 for the R isomer. In a previous work,[20] we studied the reaction of formation of one of the possible osmate products from the reactants, and characterized an intermediate and a transition state along the reaction path. In the present paper, the study is extended to all the possible isomeric products, the barrier for each path being characterized by the energy of its transition state. The energies of the more relevant transition states are then decomposed and compared term by term to quantify the different factors defining the selectivity. Different from previous studies, this work is carried out through a first principles method such as IMOMM, with full optimization of each of the transition states.

The paper is organized in different sections. After this introduction and the computational details, the sections are concerned with the definition of the possible paths, the determination of the region of entry of the olefin, and the elucidation of the preferred orientation of the olefin within this region. The final sections contain an overall view of the mechanism of selectivity and the conclusions.

Computational Details

IMOMM calculations[16] were performed with a program built from modified versions of the standard programs Gaussian 92/DFT[22] for the quantum mechanics part and MM3(92)[23] for the molecular mechanics part. The molecular orbitals calculations were carried out on the $OsO_4(NH_3)$ + CH_2CH_2 fragment at the Becke3LYP level.[24] The basis set was LANL2DZ for Os,[25] 6-31G(d) for O,[26] and 6-31G for N, C, and H.[26a] Molecular mechanics calculations used the MM3(92) force field,[27] with van der Waals parameters for Os taken from the UFF force field.[28] Torsional contributions involving dihedral angles with the metal atom in the terminal position were set to zero. All geometrical parameters were optimized except the bond distances connecting the QM and MM parts, which were kept constant: N−H (1.015 Å), C−H (1.101 Å) in the ab initio part and N−C (1.448 Å), C−C (1.434 Å) in the molecular mechanics part.

The computational algorithms applied are efficient in the search of single local minima, but they are not capable of carrying out a conformational search, *i.e.*, the search for the most stable of all possible local minima. Because this limitation could be critical in a system with so many atoms, special care was taken in the choice of the conformation of the cinchona ligand. Our starting geometry for the ligand was taken from previous experimental (X-ray and NMR) and theoretical studies (MM) on both the isolated and complexed ligand.[11,14,29,30] Furthermore, in a selected case, to be mentioned below, an additional conformation was also tested.

(17) (a) Matsubara, T.; Maseras, F.; Koga, N.; Morokuma, K. *J. Phys. Chem.* **1996**, *100*, 2573. (b) Svensson, M.; Humbel, S.; Morokuma, K. *J. Chem. Phys.* **1996**, *105*, 3654. (c) Matsubara, T.; Sieber, S.; Morokuma, K. *Int. J. Quantum Chem.* **1996**, *60*, 1101. (d) Froese, R. D. J.; Morokuma, K. *Chem. Phys. Lett.* **1996**, *263*, 393. (e) Coitiño, E. L.; Truhlar, D. G.; Morokuma, K. *Chem. Phys. Lett.* **1996**, *259*, 159.

(18) (a) Barea, G.; Maseras, F.; Jean, Y.; Lledós, A. *Inorg. Chem.* **1996**, *35*, 6401. (b) Ujaque, G.; Maseras, F.; Eisenstein, O. *Theor. Chem. Acc.* **1997**, *96*, 146. (c) Ogasawara, M.; Maseras, F.; Gallego-Planas, N.; Kawamura, K.; Ito, K.; Toyota, K.; Streib, W. E.; Komiya, S.; Eisenstein, O.; Caulton, K. G. *Organometallics* **1997**, *16*, 1979. (d) Maseras, F.; Eisenstein, O. *New J. Chem.* **1998**, *22*, 5. (e) Ujaque, G.; Cooper, A. C.; Maseras, F.; Eisenstein, O.; Caulton, K. G. *J. Am. Chem. Soc.* **1998**, *120*, 361. (f) Barea, G.; Lledós, A.; Maseras, F.; Jean, Y. *Inorg. Chem.* **1998**, *37*, 3321.

(19) Ujaque, G.; Maseras, F.; Lledós, A. *Theor. Chim. Acta* **1996**, *94*, 67.

(20) Ujaque, G.; Maseras, F.; Lledós, A. *J. Org. Chem.* **1997**, *62*, 7892.

(21) Corey, E. J.; Noe, M. C. *J. Am. Chem. Soc.* **1996**, *118*, 319.

(22) Frisch, M. J.; Trucks, G. W.; Schlegel, H. B.; Gill, P. W. M.; Johnson, B. G.; Wong, M. W.; Foresman, J. B.; Robb, M. A.; Head-Gordon, M.; Replogle, E. S.; Gomperts, R.; Andres, J. L.; Raghavachari, K.; Binkley, J. S.; Gonzalez, C.; Martin, R. L.; Fox, D. J.; Defrees, D. J.; Baker, J.; Stewart, J. J. P.; Pople J. A. *Gaussian 92/DFT*; Gaussian Inc.: Pittsburgh, PA, 1993.

(23) Allinger, N. L. *mm3(92)*; QCPE: Bloomington, IN, 1992.

(24) (a) Becke, A. D. *J. Chem. Phys.* **1993**, *98*, 5648. (b) Lee, C.; Yang, W.; Parr, R. G. *Phys. Rev. B* **1988**, *37*, 785. (c) Stephens, P. J.; Devlin, F. J.; Chabalowski, C. F.; Frisch, M. J. *J. Phys. Chem.* **1994**, *98*, 11623.

(25) Hay, P. J.; Wadt, W. R. *J. Chem. Phys.* **1985**, *82*, 299.

(26) (a) Hehre, W. J.; Ditchfield, R.; Pople, J. A. *J. Chem. Phys.* **1972**, *56*, 2257. (b) Hariharan, P. C.; Pople, J. A. *Theor. Chim. Acta* **1973**, *28*, 213.

(27) (a) Allinger, N. L.; Yuh, Y. H.; Lii, J. H. *J. Am. Chem. Soc.* **1989**, *111*, 8551. (b) Lii, J. H.; Allinger, N. L. *J. Am. Chem. Soc.* **1989**, *111*, 8566. (c) Lii, J. H.; Allinger, N. L. *J. Am. Chem. Soc.* **1989**, *111*, 8576.

(28) Rappé, A. K.; Casewit, C. J.; Colwell, K. S.; Goddard, W. A., III; Skiff, W. M. *J. Am. Chem. Soc.* **1992**, *114*, 10024.

(29) Kolb, H. C.; Andersson, P. G.; Sharpless, K. B. *J. Am. Chem. Soc.* **1994**, *116*, 1278.

(30) Berg, U.; Aune, M.; Mattson, O. *Tetrahedron Lett.* **1995**, *36*, 2137.

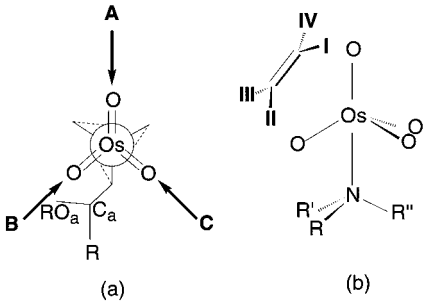

Figure 1. Definition of the possible reaction paths in the IMOMM calculations. (a) Top view along the O−Os−N axis showing the three different regions (**A**, **B**, **C**) of approach of the olefin. (b) Side view perpendicular to the O−Os−N axis showing the four possible positions (**I**, **II**, **III**, **IV**) of the phenyl ring of styrene.

Table 1. Relative IMOMM(Becke3LYP:MM3) Energies (kJ·mol^{-1}) of the Transition States Associated to Each of the 12 Possible Reaction Paths[a]

		A	B	C
I	QM	−3.0	0.00	−0.2
	MM	23.3	0.00	27.5
	total	20.2	0.00	27.3
II	QM	−1.7	−0.4	1.2
	MM	28.7	22.9	19.5
	total	27.0	22.6	20.7
III	QM	−2.4	−2.7	3.9
	MM	26.9	3.1	35.2
	total	24.5	0.4	39.0
IV	QM	−1.7	−1.5	1.1
	MM	21.3	12.6	19.2
	total	19.6	11.1	20.4

[a] All energies are relative to that of the lowest transition state (**B-I**). Reaction paths are labeled following Figure 1.

Twelve Possible Pathways

To investigate the transition state associated with the formation of the osmate ester, one must take into account all the different ways in which olefin **2** can approach catalyst **1**. These different paths are classified according to the criteria depicted in Figure 1. Figure 1a shows the possible regions of approach of the olefin to the catalyst from a top view along the O−Os−N axis. Catalyst **1** has a trigonal bipyramidal coordination around the metal, with the O(Os) and C(N) substituents taking a staggered orientation with respect to the Os−N bond. The alkene forms bonds with the axial and with one of the three equatorial oxygen atoms. Since the three equatorial oxygen atoms are not equivalent, the approach to each of them defines therefore a distinct family of reaction paths, which we have labeled as "regions" **A**, **B**, and **C**, following the same nomenclature proposed by Sharpless and co-workers.[29] A second question is the placement of the phenyl substituent of the styrene substrate, which is illustrated in Figure 1b. The phenyl can replace any of the four hydrogens of ethylene, giving rise to four different "orientations" of the substrate, which we have labeled as **I**, **II**, **III**, and **IV**. The joint consideration of the three regions of approach and the four possible positions of the phenyl ring per region yield a total of twelve different pathways. The overall selectivity of the reaction depends on the orientation of the substrate. When the orientation is **I** or **III**, the final diol product is the R enantiomer, and when it is **II** or **IV** the S product is obtained.

Each of these twelve possible paths were theoretically characterized through the location of the corresponding transition state, their energies being collected in Table 1. The energies are relative to that of the lowest transition state, **B-I**, to emphasize the comparison between different paths. The values always should be *ca*. 25 kJ·mol^{-1} above those of the corresponding intermediates.[20] It is noteworthy that each of the twelve calculations converged to a different saddle point in the potential energy hypersurface, with a negative eigenvalue in the approximate Hessian, and with the corresponding eigenvector having large components in the O−C distances. There are therefore twelve different geometries to be analyzed, each with its corresponding energy. The reaction is in any case going to proceed mostly through the lowest energy saddle point, which will be the true transition state of the reaction.

The nature of the lower energy paths and the factors defining their preference are going to be discussed in detail in the next sections, but a first general discussion on Table 1 can already be made here. The decomposition of the energy in quantum mechanics (QM) and molecular mechanics (MM) parts shows that the differences are mostly in the MM part (differences of up to 35.2 kJ·mol^{-1}) with differences in the QM part being much smaller (a maximum difference of 6.9 kJ·mol^{-1}). This is an important point, because it proves that *the enantioselectivity is governed by the steric interactions between the catalyst and the olefin*.

The fact that the differences between the several transition states are mostly in the MM part may put into question the real need of the IMOMM method for this problem. The application of the simpler MO-then-MM approach[17a,31] has however serious problems related to the nature of the more stable arrangement of hydrogen substituents resulting from MO calculation, and test calculations of this type yielded unsatisfactory results.

Region of Entry of the Substrate: A, B, or C?

The discussion on which are the lower energy paths is divided in two parts. In this section, the region of entry of the olefin is analyzed. It can be seen in Table 1 that the three lower energy saddle points correspond to region **B**: **B-I**, **B-III**, and **B-IV**, with relative energies of 0.0, 0.4, and 11.1 kJ·mol^{-1}, respectively. Although the other saddle point corresponding to this region, **B-II**, is somehow higher in energy at 22.6 kJ·mol^{-1}, there is no doubt that this is the preferred region of entry for the olefin. The lowest energy saddle points for regions **A** and **C** are at *ca*. 20 kJ·mol^{-1} above that for region **B**. This computed preference for region **B** is in full agreement with the suggestions emerging from kinetic observations by Sharpless and coworkers.[29] In a thorough study on the $(DHQD)_2PHAL{\cdot}OsO_4$ ($(DHQD)_2PHAL$ = bis(dihydroquinidine)phtalazine) catalyst, they found that the nature of substituents at C_a and, especially, O_a (Figure 1a), affects substantially the rate of the reaction. These substituents are likely to affect mostly the **B** region.

The fact that region **B** is preferred over region **A** has a direct consequence on the nature of the steric interactions between catalyst and substrate. It is clear from Figure 1a that region **A** has the least steric crowding. Therefore the magnitude of steric interactions must be smaller in region **A** than in region **B**. The fact that the energy of the saddle points is lower in region **B** can only mean that the steric interactions are of an attractive nature. This is in fact also fully consistent with the existence of an intermediate in the reaction path.[20]

B is therefore the preferred region for the reaction, and the discussion on enantioselectivity in the next section will be carried out only within this region. It is, however, worth noticing that enantioselectivity happens precisely in the way it happens

(31) (a) Kawamura-Kuribayashi, H.; Koga, N.; Morokuma, K. *J. Am. Chem. Soc.* **1992**, *114*, 8687. (b) Maseras, F.; Koga, N.; Morokuma, K. *Organometallics* **1994**, *13*, 4008.

because the reaction goes through region **B**. If the reaction went through the less sterically hindered region **A**, there would be almost 50% of R and S products, coming from the very close relative energies of the saddle points corresponding to isomers **A-I** (20.2 kJ·mol^{-1}) and **A-IV** (19.6 kJ·mol^{-1}). If the reaction were to go through path **C** the main product would actually be the S isomer (either through path **C-IV**, 20.4 kJ·mol^{-1}, or **C-II**, 20.7 kJ·mol^{-1}), with a minor nonneglectable quantity of the R product (through path **C-I**, 27.3 kJ·mol^{-1}). Therefore, the overall R selectivity of the reaction is intimately related to the fact that it goes through region **B**.

Orientation of Substrate within Region B: I, II, III, or IV?

After showing that the reaction goes through region **B**, the analysis shifts to which is the preferred orientation of the substrate within this region. This is the point where selectivity is decided, since isomers **I** and **III** lead to the R product, and isomers **II** and **IV** lead to the S product. The results, collected in Table 1, are conclusive, the R isomer will be formed, because the two lowest energy saddle points (with an energy difference of only 0.4 kJ·mol^{-1} between them) are **B-I** and **B-III**.

Experimental results on this system show that the product is the R enantiomer, being therefore in good agreement with these calculations. The agreement reaches even the value of the enantiomeric excess. Its computational estimation relies on some hypothesis, namely that the ratio of the products follows that of a Maxwell−Boltzmann distribution based on the internal energies of the transition states at 0 K. Accepting this hypothesis, one obtains a ratio of reaction paths of 53.5% through path **B-I**, 45.9% through path **B-III**, and 0.6% through path **B-IV**. Since both **B-I** and **B-III** give the R isomer, this would mean a proportion of 99.4% of R product, in good agreement with the reported experimental enantiomeric excess of 96.[11,21] This is indeed a quite remarkable success for the first-principles IMOMM method.

Since this is the point where the enantioselectivity is decided, the properties of these saddle points are analyzed in some detail. The optimized structures of the three lower energy isomers, **B-I**, **B-III**, and **B-IV**, are presented in Figures 2, 3, and 4, respectively. Before entering in the discussion of each of the geometries it is worth mentioning that we confirmed that **B-III** was in its lowest energy conformation through an additional calculation. This geometry was specially doubtful because a similar geometry had been proposed from molecular mechanics calculations on the [2 + 2] reaction mechanism[14] but with a slightly different conformation. We performed a full search of the saddle point starting from the alternative conformation of the cinchona group and reached a saddle point that was 9.3 kJ·mol^{-1} above the structure for **B-III** presented above. This alternative structure is presented in Figure 5, and the difference from the most stable structure (Figure 3) is in the arrangement of the quinoline group labeled as "quinoline A", in particular a rotation of *ca*. 180° of the dihedral angle around the C−C bond connecting the quinoline to the rest of the catalyst. This alternative conformation will not be discussed any further because of its higher energy.

From Table 1 it is clear that most of the energy difference between the different saddle points is in the MM part, with the QM part being quite similar. Additional calculations were carried out to analyze the different contributions to the MM energy. In the first place, the interaction energy between substrate and catalyst is separated into binding and distorsion contributions. To do this, the process of formation of each saddle point from the separate reactants is divided into two imaginary steps: (i) the first step where the catalyst and the substrate at infinite distance are distorted to the geometry they have in the saddle point (distortion energy) (ii) and the second step where they are put together to yield the saddle point structure (binding energy). The results of this analysis are collected in Table 2.

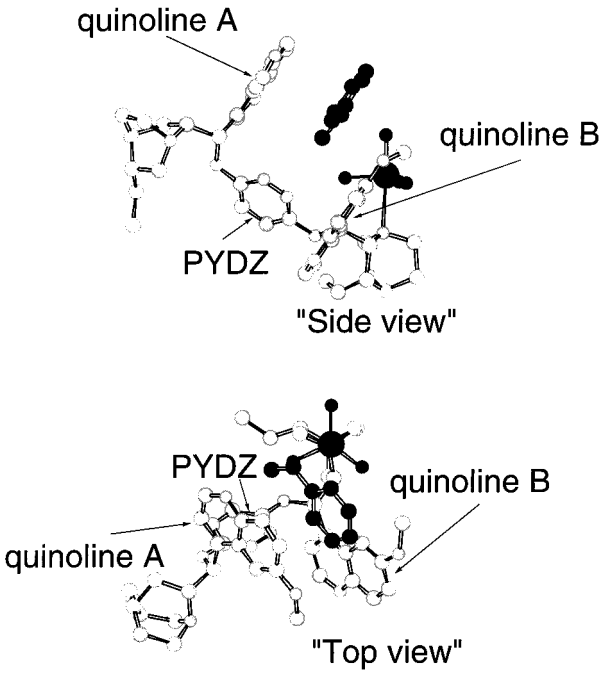

Figure 2. Two different views of the IMOMM (Becke3LYP:MM3) optimized transition state **B-I**. The styrene substrate and the OsO_4 unit are highlighted in black.

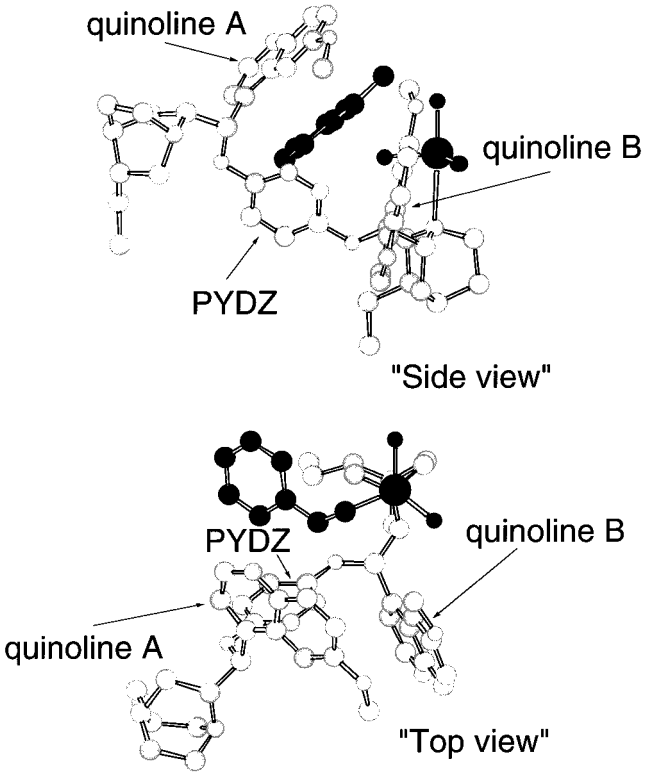

Figure 3. Two different views of the IMOMM(Becke3LYP-MM3) optimized transition state **B-III**. The styrene substrate and the OsO_4 unit are highlighted in black.

It is worth noticing that most interaction energies are negative, a result consistent with the connection of the saddle points to

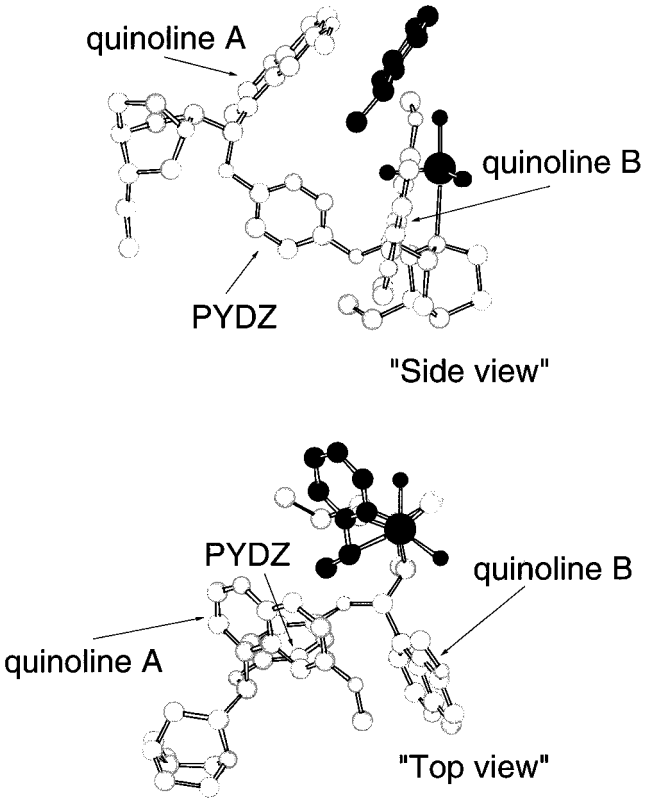

Figure 4. Two different views of the IMOMM(Becke3LYP:MM3) optimized transition state **B-IV**. The styrene substrate and the OsO_4 unit are highlighted in black.

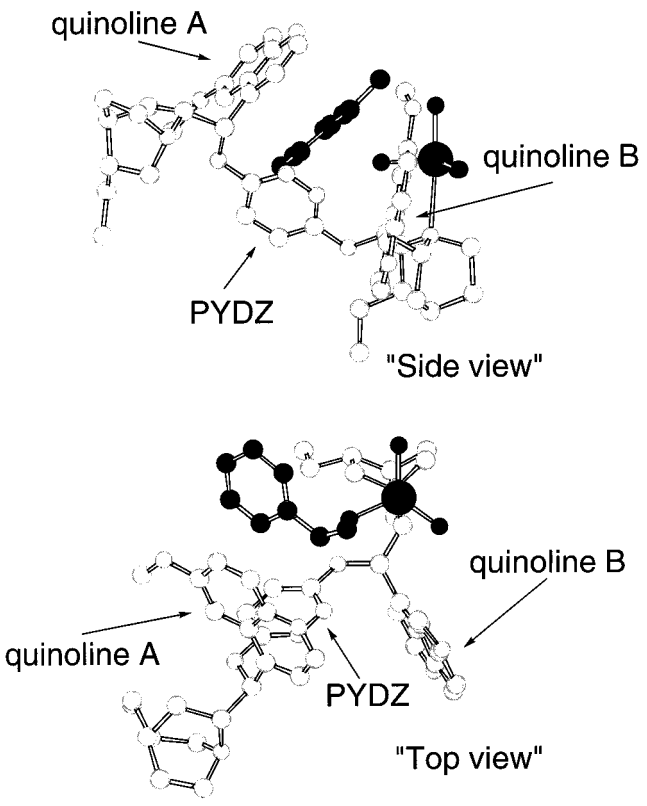

Figure 5. Two different views of the IMOMM(Becke3LYP:MM3) optimized structure of the alternative higher energy conformer of transition state **B-III**. The styrene substrate and the OsO_4 unit are highlighted in black.

lower energy intermediates and not directly to the reactants.[20] The table shows how the final values of interaction energy are obtained through the addition of terms of different magnitude. For instance, while **B-I** and **B-III** have practically the same interaction energy, **B-I** has larger absolute values than **B-III** for both the distortion and binding terms by more than 10 kJ·mol^{-1}, both differences being finally compensated because they have opposite sign. Therefore, the interaction between catalyst and substrate is larger in **B-I**, but it is only reached after a larger distortion in the structure of the catalyst. The reasons for the poor stability of the saddle points potentially leading to the S product, **B-II** and **B-IV**, also appear to be different. In the case of **B-II** there is a very large distortion energy of 75.7 kJ·mol^{-1}, while in the case of **B-IV** the problem is the too small binding energy of −56.3 kJ·mol^{-1}.

Table 2. Decomposition of the Interaction Energy (E_i) in Binding Energy (E_b) and Distortion Energy (E_d) for Each of the IMOMM(Becke3LYPL:MM3) Saddle Points Associated to Reaction Paths through Region **B**[a]

		E_i	E_d	E_b
I	QM	19.6	50.0	−30.4
	MM	−33.5	14.3	−47.8
	total	−13.8	64.3	−78.2
II	QM	19.3	51.2	−31.9
	MM	−10.5	24.9	−35.4
	total	8.7	75.7	−67.3
III	QM	17.0	48.8	−31.8
	MM	−30.4	5.5	−35.9
	total	−13.4	54.3	−67.7
IV	QM	18.1	47.1	−29.0
	MM	−20.9	6.5	−27.4
	total	−2.7	53.6	−56.3

[a] All energies are in kJ·mol^{-1}.

The analysis can be further refined to see which are the specific parts of the catalyst contributing to the binding energy. This can be done because the IMOMM partition in this particular system leaves most of the binding between catalyst and substrate in the MM part. The MM binding energies oscillate widely between −27.4 and −47.8, while the QM change is very small in comparison, with changes only between −29.0 and −31.9 kJ·mol^{-1}. Furthermore, the difference is in the so called van der Waals term. The dominance of this particular term can be surprising, but it must be said that it is very likely affected by the choice of the MM3 force field. Other force fields grant a lesser importance to van der Waals terms and give more weight to electrostatic contributions, for instance. If such other force fields had been applied the decomposition would likely be substantially different, and other terms should be more important in defining the difference. In any case, the total difference would have to be similar, as far as the different force fields are properly describing the same chemically reality. So this result is merely used in the sense that the more significant MM contributions correspond to what MM3 calls van der Waals interactions, without entering in the real chemical meaning of such terms.

Whatever the real chemical meaning of the MM3 van der Waals term, it has the very useful property for analysis of being defined by interactions between pairs of atoms. Using this fact, the interaction between the substrate atoms and those of the catalyst has been divided in different blocks for the four saddle points of region **B**, and the results are collected in Table 3. The different parts of the catalyst that have been considered are the two quinoline rings sandwiching the styrene substrate, labeled arbitrarily as quinoline A and quinoline B, the pyridazine spacer PYDZ, the OsO_4 unit, and the rest of the molecule. This classification is closely related to the analysis of the binding pocket that has been carried out previously by the groups of

Table 3. Decomposition of the MM3 van der Waals Interaction Energy between Substrate and Catalyst for Each of the IMOMM(Becke3LYP:MM3) Saddle Points Associated to Reaction Paths through Region B[a]

	quinoline A	quinoline B	PYDZ	OsO_4	rest	total
I	25.4 (53)	9.7 (20)	5.5 (12)	2.0 (4)	5.1 (11)	47.8
II	7.3 (21)	9.5 (27)	9.6 (27)	0.5 (1)	8.4 (24)	35.4
III	15.2 (42)	4.2 (12)	7.9 (22)	1.0 (3)	7.7 (21)	35.9
IV	15.7 (57)	4.1 (15)	3.0 (11)	1.4 (5)	3.2 (12)	27.4

[a] The labeling of the areas of the catalyst is indicated in Figures 2 to 4. Energies are indicated in kJ·mol^{-1}, with percentages with respect to total interaction in parentheses.

Corey[11,21] and Sharpless.[14,29,32,33] Quinolines A and B define the parallel walls of the U-shaped binding pocket, with the pyridazine defining the bottom wall.

The results, collected in Table 3, allow a quantification of the relative importance of the different regions of the catalyst in the stereoselectivity of the reaction. The first result worth remarking on is how three of the considered fragments, quinoline A, quinoline B, and PYDZ, always account for more than 75% of the MM interaction between catalyst and substrate, showing the appropriateness of the analysis in terms of these fragments. The interactions between substrate and the two quinoline rings are face-to-face stacking interactions and the interaction between styrene and pyridazine is face-to-edge. This type of interaction is well characterized in other chemical systems,[34] and its existence is therefore not surprising here. It is moreover in agreement with the previously postulated importance of π-π interactions in this particular system.[20]

As for their relative importance, it is clear from Table 3 that the most important interaction for **B-I**, **B-III**, and **B-IV** is the face-to-face interaction with quinoline A. Quinoline A is the one further away from the metal center, and its importance is consistent with the higher selectivity associated with the second generation catalysts. The dominance of the face-to-face interaction with quinoline A does not mean in any case that the face-to-face interaction with quinoline B and the face-to-edge interaction with the pyridazine is neglectable. This is still sufficient to allow for the enantioselectivity of first-generation catalysts, and can have a decisive importance in distinguishing between some paths.

Despite the fact that they have almost the same energy and lead to the same product, saddle points **B-I** and **B-III** have a series of differences. Saddle point **B-I** is the one that had been considered in previous analysis of the [3 + 2] mechanism,[11,20] and indeed has the lowest energy. It has a good overlap between quinoline A and styrene (Figure 2), reflected in the largest catalyst−substrate binding energy of −78.2 kJ·mol^{-1} (Table 2). However, this is accomplished through a quite important distortion energy of 64.3 kJ·mol^{-1}. Saddle point **B-III**, a variant of which had been proposed as active in the [2 + 2] mechanism,[14,29] had an energy only 0.4 kJ·mol^{-1} higher. In this case, the interaction energy is less favorable (−67.7 kJ·mol^{-1}), but the distortion from the reactant structure is also significantly smaller (54.3 kJ·mol^{-1}). In what concerns the interaction with the different regions of the catalyst (Table 3), for both **B-I** and **B-III** the main interaction is the face-to-face interaction styrene−quinoline A, with 53% in the case of **B-I** and 42% in the case of **B-III**. For the other interactions, it is worth noticing that the role of quinoline B is more important in **B-I** (20%), while the face-to-edge interaction with PYDZ is more important in **B-III** (22%). It is clear that **B-III** is a competitive path for the reaction also in the [3 + 2] mechanism, and will have to be taken into account in further studies of this type of systems.

The key to the selectivity is in any case the comparison of the previously discussed **B-I**, **B-III** saddle points, leading to the R product, with the **B-IV** saddle point leading to the S product. The experimental formation of a very minor proportion of S product must come from **B-IV** (11.1 kJ·mol^{-1} above **B-I**), since **A-IV**, which is the following S-type saddle point, appears at much higher energy (22.6 kJ·mol^{-1}). The structure of saddle point **B-IV** is presented in Figure 4. The distorsion energy is practically the same as in **B-III** (53.6 *vs* 54.3 kJ·mol^{-1}), but the binding energy is smaller (−56.3 *vs* −67.7 kJ·mol^{-1}). The pattern of relative weight of the interactions with different parts of the catalyst is not very different from that of **B-I**, **B-III**, with a clear dominance of quinoline A (with 57% in this case). It is worth noticing that a substantial part of the difference in absolute interaction energies between **B-III** and **B-IV** is in the interaction with pyridazine. The interaction styrene−PYDZ is worth 7.9 kJ.mol−1 in **B-III** and only 3.0 in **B-IV**, while differences between the interactions of the substrate with quinolines A and B are 0.5 kJ·mol^{-1} at most. Therefore, although the interaction with quinoline A is still the largest, the subtle differences leading to enantioselectivity can be in other areas of the catalyst.

In summary, it is clear that although the results can be rationalized a posteriori, it is difficult to know a priori which are the relative weights of the different factors contributing to the decision of the selectivity. In this concern, the performance of quantitative theoretical calculations can be extremely helpful.

Relationship to the Mechanism of Stereoselectivity with Other Substrates

Our calculations on the mechanism of the reaction of styrene with $(DHQD)_2PYDZ{\cdot}OsO_4$ reproduce properly the experimental stereoselectivity and provide a detailed explanation for its origin, but also have implications on the general mechanism of stereoselectivity for other substrates and catalysts. In this section we try to place these results into the context of known data and previous mechanistic proposals for these processes.

One point worth commenting on is that our results indicate that the reaction goes almost indistinctly through two different paths (**B-I** and **B-III**) leading to the same product. Remarkably, variations of both paths had already been proposed, but they have been used as supporting evidence for two opposing mechanistic proposals, the [3 + 2] and [2 + 2] mechanisms. Now that the reaction has been proved to take place through the [3 + 2] mechanism, it is not surprising to find that the reaction can go through the **B-I** path, which previously had been associated with this mechanism.[11] But it was more unexpected to find a competitive energy for path **B-III**, a variety of which had been used to support the now disproved [2 + 2] mechanism.[29] The two paths that had presented as opposed, therefore happen to complement each other.

The relative energies for the four possible orientations of the styrene within region B (Table 1) suggest that, with this catalyst, a trans-disubstituted olefin should give higher stereoselectivity, and that a cis-disubstituted olefin should give a lower one. Both observations are in agreement with previous experimental reports.[1,35] The dihydroxylation of cis-disubstituted olefins is in fact efficiently catalyzed only by osmium complexes contain-

(32) Norrby, P.-O.; Becker, H.; Sharpless, K. B. *J. Am. Chem. Soc.* **1996**, *118*, 35.

(33) Nelson, D. W.; Gypser, A.; Ho, P.-T.; Kolb, H. C.; Kondo, T.; Kwong, H.-L.; McGrath, D. V.; Rubin, A. E.; Norrby, P.-O.; Gable, K. P.; Sharpless, K. B. *J. Am. Chem. Soc.* **1997**, *119*, 1840.

(34) (a) Jorgensen, W. L.; Severance, D. L. *J. Am. Chem. Soc.* **1990**, *112*, 4768. (b) Graf, D. D.; Campbell, J. P.; Miller, L. L.; Mann, K. R. *J. Am. Chem. Soc.* **1996**, *118*, 5480. (c) Graf, D. D.; Duan, R. G.; Campbell, J. P.; Miller, L. L.; Mann, K. R. *J. Am. Chem. Soc.* **1997**, *119*, 5888.

ing a completely different cinchona ligand from the one used in our calculations.[1] Results reported in Table 3 concerning the effect of different areas of the catalyst are also in overall agreement with the empirical mnemonic device to predict stereoselectivity derived by Sharpless and co-workers from extensive experimental data.[1,29]

Extrapolation of the results obtained with the $(DHQD)_2PYDZ \cdot OsO_4 + H_2C{=}CH(Ph)$ system likely produces certain explanations to a number of observed experimental features, but definite answers can only come from calculations on each specific system. In particular, further calculations could provide a precise characterization of the origin of the differences observed between six classes of olefin substrates,[36] which are already somehow suggested in Table 1. Explanation of other experimental results would require new calculations. This is the case for the behavior of substrates with only saturated chains attached to the olefin,[21] or larger substrates where the aromatic substituent is far away from the double bond.[11] The performance of such calculations exceeds however the scope of the present paper, since although the method applied permits the study of systems which could not be treated before, the calculations still require a considerable amount of computational and human effort.

A final point concerning the relationship of the present theoretical results with experimental data is the fact that our calculations completely neglect solvation effects. This is obviously a limitation in the reproduction of the experiment, where a certain dependence of the enantiomeric excess on the nature of the solvent has in fact been reported.[37] On the other hand, this situation has the advantage of allowing the computational experiment of carrying out the reaction without solvent. The results are conclusive in the sense that, for this particular substrate and catalyst, the calculation in the absence of solvent agrees well with the experimental observation for the dihydroxylation under conventional conditions.

(35) Sharpless, K. B.; Amberg, W.; Beller, M.; Chen, H.; Hartung, J.; Kawanami, Y.; Lübben, D.; Manoury, E.; Ogino, Y.; Shibata, T.; Ukita, T. *J. Org. Chem.* **1991**, *56*, 4585.

(36) Andersson, P. G.; Sharpless, K. B. *J. Am. Chem. Soc.* **1993**, *115*, 7047.

(37) Corey, E. J.; Noe, M. C. *J. Am. Chem. Soc.* **1993**, *115*, 12579.

Conclusions

The origin of enantioselectivity in the asymmetric dihydroxylation of styrene catalyzed by $(DHQD)_2PYDZ \cdot OsO_4$ has been analyzed through theoretical calculations with the IMOMM method. The twelve different possible paths of approach have been examined and characterized through the energy of these transition states. The two lower energy paths are associated with the R isomer, and the lower path leading to the S isomer is 11.1 $kJ \cdot mol^{-1}$ higher in energy. This would lead to a 99.4 formation of the R product, in good agreement with the experimental observation of an enantiomeric excess of 96.

The analysis of the corresponding transition states leads to the identification of the factors governing the selectivity. The leading role is played by stacking interactions between aromatic rings of olefin and catalyst. These are the plane-to-plane interactions between the substrate and the two quinoline rings of the catalyst, as well as the plane-to-edge interaction between the substrate and the pyridazine ring. The larger contribution corresponds to the interaction with the quinoline ring of the second subunit of the "dimeric" catalyst, which has been labeled as quinoline A, accounting for *ca*. 50% of the total stabilization.

Acknowledgment. This paper is dedicated to Prof. Keiji Morokuma on the occasion of his 65th birthday. Financial support from the Spanish DGES through Project No. PB95-0639-CO2-01 is acknowledged. FM thanks the French CNRS for financial support as a Research Associate.

JA9816335